Research Article

Genomic regions targeted by DNA topoisomerase IIβ frequently interact with a nuclear scaffold/matrix protein hnRNP U/SAF-A/SP120

Mary Miyaji*[,1], Ryohei Furuta[1], Kuniaki Sano, Kimiko M. Tsutsui, and Ken Tsutsui*
Department of Neurogenomics, Graduate School of Medicine, Dentistry and Pharmaceutical Sciences, Okayama University, 2-5-1 Shikata-cho, Kita-ku, Okayama 700-8558, Japan

[1]These authors equally contributed to this work.

*Corresponding authors:
Department of Neurogenomics, Graduate School of Medicine, Dentistry and Pharmaceutical Sciences, Okayama University, 2-5-1 Shikata-cho, Kita-ku, Okayama 700-8558, Japan. Phone: +81-86-235-7097, Fax: +81-86-235-7103.
E-mail: tsukken@cc.okayama-u.ac.jp (K.T.), mmiyaji@md.okayama-u.ac.jp (M.M.)

Running Title: Genomic regions targeted by topoisomerase IIβ

Keywords:

- **neuronal differentiation**
- **topoisomerase II**
- **nuclear scaffold/matrix**
- **hnRNP U**

Total number of text figures: 6

Contract grant sponsor: Ministry of Education, Science, Sports and Culture, Japan.
Contact grant numbers: 21710197 and 26650125 to M.M.; 23310133 to K.T.

ABSTRACT

Type II DNA topoisomerases (topo II) play critical roles in some cellular events through repeated cleavage/rejoining of nuclear DNA. The β isoform (topo IIβ) is essential for the transcriptional induction of neuronal genes in terminal differentiation. Genomic sites targeted by the enzyme are nonrandom. Although previous studies have claimed that topo II cleavage sites are close to the nuclear scaffold/matrix attachment region (S/MAR), it is still unclear whether this view can be generalized. We report here that a library of cloned genomic DNA fragments targeted by topo IIβ *in vivo* frequently contains S/MAR and binding sites for hnRNP U/SAF-A/SP120. Binding assays *in vitro* showed that a large proportion of the target DNAs bound to SP120 but their affinity to the nuclear scaffold/matrix varied significantly. Topo IIβ targets were extremely AT-rich and often located in gene-poor long intergenic regions (so-called gene desert) that are juxtaposed to long genes expressed in neurons under differentiation. Sequence analysis revealed that topo IIβ targets are not just AT-rich but are enriched with short tracts of A's and T's (termed A/T-patches). Their affinity to the nuclear scaffold/matrix showed a moderate positive correlation with the coverage rate of A/T-patches. The results suggest that the interaction of topo IIβ/SP120 with target regions modulates their proximity to the nuclear scaffold/matrix in a dynamic fashion and that A/T-patch is a sequence motif assisting this process.

Unlike the α isoform, which is involved in chromosomal segregation in proliferating cells, the β isoform of DNA topoisomerase II (topo IIβ) is closely correlated with transcriptional regulation in differentiating neuronal cells [Tsutsui et al., 2001b; Lyu et al., 2006; Sano et al., 2008]. Another line of studies has shown that topo IIβ is involved in transcriptional activation of some inducible genes through transient double-stranded DNA breakage events around promoters [Ju et al., 2006; Perillo et al., 2008].

In the rat cerebellar tissue, neuronal differentiation culminates at around 10 days after birth (P10), when topo IIβ is expressed mostly in the post-migratory granule neurons in the granule layer [Tsutsui et al., 2001a]. By incubating the cerebellar tissue with etoposide, a topo II-specific poison that produces covalent linkage between the enzyme and target DNA, we have shown that topo IIβ is highly accessible to DNA in the nucleoplasm but it becomes less accessible to DNA around P20, being sequestered in nucleoli [Tsutsui et al., 2001b]. In the same work we established a primary culture of granule neurons from the P8 cerebellum in that only cells right after the final cell division survive and continue to differentiate *in vitro*. Using this cell system we identified a group of genes whose expression is induced depending on the topo IIβ activity during the early stage of terminal differentiation, and showed later that these genes are located at characteristic genomic regions with high AT contents [Sano et al., 2008].

In the present study, we obtained a number of DNA clones targeted by topo IIβ in the P10 cerebellum. Tissue slices incubated with etoposide were lysed and subjected to immunoprecipitation with a topo IIβ-specific antibody to concentrate DNA fragments cross-linked to the enzyme. The fragments were cloned and used to address whether these genomic regions contain interaction sites with the nuclear scaffold/matrix (scaffold/matrix associated region; S/MAR). Although it has been demonstrated that topo II action sites are closely associated with S/MARs [Cockerill and Garrard, 1986; Gasser and Laemmli, 1986], rather poor experimental evidence has been presented until now whether this notion can be generalized. The topo IIβ target regions may also be enriched in binding sites for hnRNP U/SAF-A/SP120. This protein is shown to be abundant in the nuclear scaffold/matrix (NS/M) fraction, selectively binds with S/MAR [Romig et al., 1992; Tsutsui et al., 1993], and forms an RNA-dependent molecular complex with topo IIβ [Kawano et al., 2010].

The results indicate that topo IIβ-targeted regions are AT-rich and indeed enriched with both S/MAR and SP120-binding sites. However, there was no positive correlation between SP120-binding and NS/M-binding, implying that factor(s) other than SP120 is likely to be involved in the high-affinity association with the NS/M. A significant positive correlation was observed between the NS/M-affinity and the abundance of short tracts of A's or T's in the sequence of the targeted regions. We also found that substantial topo IIβ/SP120 interaction sites are in the chromosome loop region and not restricted in the vicinity of S/MAR.

MATERIALS AND METHODS

Antibodies

Monoclonal antibodies against topo IIα (4E12) and topo IIβ (3B6) and the polyclonal antibody against SP120 were prepared as described [Kawano et al., 2010]. Rabbit control IgG was purified from preimmune serum using the MAb Trap Kit as described [Kawano et al., 2010]. Polyclonal antibody against SP120 was obtained by immunizing rabbits with a synthetic peptide GDKKRGVKRPREDH, which corresponds to amino acid residues 214-227 of rat SP120 (accession D14048). The antibody was affinity-purified with the antigenic peptide bound to Sulfolink Coupling Gel (Pierce) as described [Kawano et al., 2010].

Isolation of genomic fragments targeted by topo IIβ

All animal protocols were in accordance with the animal care and use guidelines of the Okayama University Medical School.

The cerebellum was removed from infant Wistar rats at 10 days after birth, cut into 1 mm-thick slices, and submerged in RPMI-1640 medium supplemented with 100 μM etoposide. After incubation at 37°C for 2 h in a CO_2 incubator, the tissue slices were homogenized in 3 ml of 1% sarkosyl containing 10 mM EDTA and 10 mM Tris-HCl (pH 7.6), and then CsCl was added to a final concentration of 0.5 M. The homogenate was sonicated for 1 min with a microtip (Branson sonifier model 250D) and diluted with three volumes of dilution buffer containing 0.5% Triton X-100, 0.1 M NaCl, 10 mM EDTA, 10 mM Tris-HCl (pH 7.5), and 0.5 mM phenylmethylsulfonyl fluoride

(PMSF). After centrifugation at 24,000 x g for 10 min, the supernatant was divided into two equal portions and incubated overnight at 4°C with 30 μg of antibody specific to either topo IIα or topo IIβ. The incubation was continued further at 37˚C for 1.5 h. Then, 1 mg of protein G-coupled magnetic particles was added, and the mixture was stirred gently at room temperature for 1.5 h. The particles were washed four times with dilution buffer and treated with 100 μg/ml proteinase K at 55˚C for 30 min. After magnetic separation of the particles, DNA fragments in the supernatants were purified by phenol/chloroform extractions followed by ethanol precipitation in the presence of carrier glycogen.

Cloning and sequencing of the topo IIβ targets

The immunoselected genomic DNA fragments were blunt-ended with T4 DNA polymerase and ligated to a zero-background cloning vector (pZErO™-2.1, Invitrogen) linearized with *Eco*RV. The ligation mixture was used to transform *E. coli* TOP10F' competent cells to construct the IP-DNA library. Transformants were selected on LB agar plates containing kanamycin and isopropyl-β-D-thiogalactopyranoside (IPTG). About 10^4 recombinant colonies were obtained per 1 ng of the genomic DNA. After cultivating individually in 96-well microplates, 400 clones were stored as a library in glycerol stocks at -80˚C. The library clones were revived and plasmid inserts were PCR amplified with vector primers and directly sequenced from both ends. Their genomic positions were determined on UCSC rat genome (rn3) by Blat search and the IP-DNA fragments were reconstituted by filling internal sequences from the database. Only uniquely mapped sequences with reasonable length (279 clones) were selected for analysis. Hereafter, these clones are referred to as "target clones".

As an alternative approach, plasmids were isolated from 48 clones and the inserts were sequenced (summarized in Table S1). These clones were also used for *in vitro* DNA binding assays with isolated NS/M or with purified SP120.

Quantitative assessment of the association between topo IIβ targets and the nuclear scaffold/matrix

Selective binding of cloned genomic DNA fragments to the isolated NS/M was assessed *in vitro* according to the procedure described previously [Tsutsui et al., 1993].

The NS/M preparation used in the present study is based on the nuclear extraction protocol with lithium diiodosalicylate (LIS). Plasmids selected randomly from the target library were digested with *Eco*RI and *Xho*I, end-labeled with ^{32}P, and incubated with the isolated NS/M in the presence of unlabeled competitor DNA consisting of a 20:1 mixture of sonicated *E. coli* DNA and pUC18. NS/M-associated DNA fragments were separated by centrifugation, purified, subjected to polyacrylamide gel electrophoresis, and visualized by autoradiography. A control reaction with plasmid pAR1, which harbors the 370 bp MAR fragment of the mouse Igκ gene [Cockerill and Garrard, 1986; Tsutsui et al., 1993], was always performed simultaneously and run parallel with test samples in all gels. Autoradiographic images were recorded on BAS2000 and signals were quantified using a densitometric software (BASstation). The NS/M-binding was calculated from the ratio of band intensities for the NS/M-bound DNA fragments in the presence and absence of 0.4 mg/ml unlabeled competitor DNA. Under these conditions 23% of Igκ MAR fragment was bound to the NS/M. Practically all the input ^{32}P-DNA bound to the NS/M when unlabeled competitor DNA was absent.

For the matrix-loop partitioning assay, nuclear halo was prepared from purified nuclei according to the LIS-extraction protocol [Tsutsui et al., 1988]. To separate genomic DNA into matrix-associated (M) and loop-enriched (L) fractions, the halo was digested with a restriction enzyme mixture (*Eco*RI, *Hind*III and *Pst*I) and centrifuged. *Eco*RI was omitted if the target region contained its cleavage site. DNA samples purified from the pellet (M) and supernatant (L) fractions were used as templates for PCR amplification with clone-specific primer pairs (shown in Table S1). The reaction was performed under standard conditions with 150 ng of templates and Amplitaq Gold DNA polymerase (Applied Biosystems). At the ends of 10, 15, 20, 25, and 30 cycles of amplification, the PCR products were analyzed on 1.5% agarose gel electrophoresis with visualization by ethidium bromide. Using scanned gel images, relative copy numbers of the products were determined by densitometry. The initial copy number in each fraction was deduced from the semi-logarithmic band intensity versus cycle number plots.

Preparation of recombinant His-Myc-SP120

To express SP120 in *E. coli*, pColdII-Myc-SP120 was first constructed using

PCR-generated fragment encoding rat SP120. Myc-tagged SP120 cDNA was amplified by PCR from pCMV-Myc-SP120 [Kawano et al., 2010]. The PCR product was inserted in frame between the *Nde*I/ *Xba*I sites of the pColdII expression vector that attaches a $(His)_6$ tag to inserts (Takara-Bio). *E. coli* cells (JM109) were transformed with pColdII-Myc-SP120. The cells were grown in LB medium supplemented with 100 μg/ml ampicillin at 37°C. When the culture reached OD 0.3 (600 nm), cold shock was applied at 15°C. After 30 min, 1 mM IPTG was added and continued to cultivate at 15°C overnight. The cells were then harvested by centrifugation at 3000 x g for 20 min and stored at -80°C. His-tagged protein was purified using Ni-NTA agarose beads (Qiagen) according to the manufacturer's protocol, except that 0.5 M NaCl was used at all the purification steps. Protein concentration of the final eluate was determined by SDS-PAGE followed by CBB staining and densitometry using BSA for calibration.

DNA binding assays with recombinant SP120 and topo IIβ target DNAs

His-Myc-SP120 (300 ng) was incubated at 25˚C for 30 min with 10 μl of Dynabeads protein G (Invitrogen) pre-coated with the SP120-specific polyclonal antibody in 100 μl of DNA-binding buffer containing 50 mM Tris-HCl (pH8.0), 120 mM KCl, 10 mM $MgCl_2$, 0.5 mM EDTA, 30 ng/μl BSA, 0.5 mM dithiothreitol, and 0.2 mM PMSF. Beads were then washed three times with the same buffer and incubated with 2 nM probe DNA at 25°C for 30 min under constant agitation. Probes had been prepared from the plasmids harboring topo IIβ targets or control DNA fragments by treating with appropriate restriction enzymes to cut at the insertion sites. Purified probes were used directly for the binding reaction as an equimolar mixture of test DNA fragment and vector DNA. After the reaction, beads were washed three times with the DNA-binding buffer, treated with proteinase K to release DNA, and removed by magnetic separation. The SP120-bound DNA in the supernatant was subjected to agarose gel electrophoresis, stained with ethidium bromide, and quantified by densitometry.

For fluorescein-based DNA-binding assay, probe DNAs were prepared by PCR amplification of target clones using M13 primers 5'-labeled with FITC. PCR products were purified with QIAquick (Qiagen) and DNA concentration was determined by measuring OD_{260}. Using the SP120-immobilized beads, DNA-binding reaction was

performed with 2 nM of FITC-labeled probe DNA and 10-fold molar excess of linearized pUC18 (unlabeled competitor) at 25°C for 30 min under constant agitation. The bound fraction was recovered by magnet, deproteinized with 200 μg/ml proteinase K in 12 μl of buffer containing 10 mM NaOH, 0.66% SDS and finally diluted with 10 mM NaOH to 200 μl. After magnetic removal of beads, the supernatant was subjected to fluorescence measurement on a microplate fluorometer (Genios, TECAN).

RESULTS AND DISCUSSION

Isolation of genomic targets of topo IIβ in developing neural tissue

Our previous study addressed a question where in genome topo IIβ most actively operates in developing neurons by applying a novel functional ChIP technique termed eTIP (etoposide-mediated topoisomerase immunoprecipitation) to a primary culture of cerebellar neuronal cells differentiating *in vitro* [Sano et al., 2008]. In the present study, we used similar procedure to probe topo IIβ targets in live tissue of the P10 rat cerebellum, in which the most dominant cell population is post-migratory granule neurons still differentiating in the granule layer (GL) (Fig. 1). These cells are in a later stage of development compared to the cells in primary culture [Tsutsui et al., 2001a]. Granule neurons proliferate in the outer part of external germinal layer (EGL) called mitotic zone. After final cell division, cell bodies migrate inward through molecular layer (ML) and enter GL where they continue to differentiate. Topo IIβ expression in granule cell nuclei starts to increase in the inner portion of EGL called pre-migratory zone and culminates in GL. The predominant staining of topo IIβ in GL (colored magenta in the overlay image) indicates that majority of immunoselected DNA fragments originates from these cells.

To ensure adequate reflection of *in vivo* situations, we excised live tissue slices from the P10 rat cerebellum and incubated them in a medium containing etoposide. The experimental strategy used in this study is illustrated in Fig. S1. The immunoprecipitated DNA fragments were cloned directly in a “zero-background” vector to construct a topo IIβ target library, from which randomly selected clones were sequenced and used for the binding analyses *in vitro* (summarized in Table S1). As shown in Fig. S2A, the topo II isoform expressed in this stage of development is mainly

β and topo IIα is hardly detectable. The DNA yield from the immunoprecipitates reflects the relative abundance of topo IIβ and the strong etoposide dependency corroborates the specificity of the immunoselection (Fig. S2B).

Topo IIβ targets are enriched with A/T nucleotides and A/T short tracts

Most obvious feature in the nucleotide sequence of target clones was their abundance in adenines and thymines (namely, AT-rich or low GC content). GC content distribution differs remarkably between the target and whole genome, target clones being extremely AT-rich (Fig. 2A). We looked for additional factors in the AT-richness of the targets and noticed a high occurrence of short tracts of A or T (termed A/T-patches). This is readily recognizable in the target sequence picked up as an example (Fig. S3). In the first place, however, A/T short tracts are enriched in mammalian genome with statistical significance when compared to random sequences [Dechering et al., 1998]. So, does the patch structure reflect characteristics of the target sequence and if so how does the tract length affect the efficiency? To answer these questions, we compared the $(A/T)_n$-patch coverage rates between the target and control sequences randomly selected from the rat genome (Fig. 2B). As expected, the patch coverage decreases exponentially as the patch size 'n' increases. Except for solitary A/T (n=1), the patch coverage was always higher in the target than in genomic control. Statistical significance for the coverage difference between these groups was calculated and plotted against 'n' (Fig. 2C). It appears that patches of n=2~5 can effectively discriminate topo IIβ-targeted regions from the background. Adopting this range for patch size definition, target clones were demonstrated to have higher patch coverage over whole genome with a high statistical confidence (Fig. 2D). Therefore, genomic targets of topo IIβ are not only AT-rich but are enriched with A/T-patches.

Topo IIβ targets are mapped to AT-rich and gene-poor regions in the genome

The target clones were also deviated in genomic positions with respect to genes. As compared to the whole genome, target clones showed higher tendency to locate in intergenic regions (Fig. 3A). In the previous study [Sano et al., 2008], we extracted intergenic regions from modified RefSeq database (exRefSeq) and classified them into 4 categories by using 2 parameters: regional length and GC content. In accordance with

these criteria, target clones were mapped preferentially to long and AT-rich intergenic region (termed LAIR). The preference was highly significant against whole genome (Fig. 3B). LAIRs are often juxtaposed to neuronal genes whose expression is induced by topo IIβ during development and thus suggested to be important for transcriptional regulation of adjacent genes [Sano et al., 2008]. Frequently, these genes are also long and AT-rich (thus called LA genes). LA genes are enriched in neuronal genes that are often mutated in psychic disorders like autism or schizophrenia. If topo IIβ target sites located in LAIR are involved in the regulation of adjacent genes, LAIRs targeted by topo IIβ would be more likely to be situated right next to LA genes. As shown in Fig. 3C, this is indeed the case: juxtaposition of LA genes against LAIRs containing topo IIβ target sites occurs much frequently when compared to LAIRs in general. In good agreement with this, most topo IIβ-targeted LAIRs (20 out of 21 identified in this study) were adjacent to LA genes that are expressed in mouse cerebellar tissue around this period of development (P7 to P14) [Sato et al., 2008].

Association of topo IIβ-targeted genomic fragments to the nuclear scaffold/matrix

An *in vitro* binding assay in the presence of nonspecific competitor DNA successfully estimated relative affinities of the target clones toward isolated NS/M in a quantitative manner (Fig. 4A-C). Whole plasmid DNA was used for the assay after digesting with restriction enzymes to liberate inserts. The resulting fragments were end-labeled with ^{32}P and the NS/M-bound fragments were detected by autoradiography. To assess the optimal competitor amount, randomly selected plasmids were subjected to a pilot experiment with varying doses of competitor DNA (Fig. 4A). Amounts of NS/M-bound fragments reflected their relative affinities to the NS/M. Fig. 4B shows the autoradiograms for 37 target clones analyzed at a fixed competitor dose that achieves complete suppression of vector binding but variable binding of topo IIβ target fragments. The frequency distribution of the resulting NS/M-binding (percent of input) implies that target clones are composed of a variety of populations with different levels of affinity to the NS/M (Fig. 4C). As abundance of A/T-patches in the target clones may have some correlation with their affinity to the NS/M, the NS/M-binding was plotted against the patch coverage rates (Fig. 4D). A significant positive correlation was discernible between these factors ($R=0.472$, $P<0.01$), suggesting that the patch structure

is also involved in the interaction with the NS/M.

Association of the target clones to the NS/M was examined by an alternative method [Chavali et al., 2011], which was referred as ‘matrix-loop partitioning assay’. This method estimates whether a particular genomic region is close to or distant from the matrix-attachment point of chromosomal loops [Mirkovitch et al., 1984; Iarovaia et al., 2005; Tsutsui et al., 2005]. The partition ratio of matrix versus loop fractions (M/L) was first determined for representative target clones by PCR amplification with clone-specific primer pairs (Table S1 and Fig. 5A). The M/L ratio was then converted to the percent DNA associated with the matrix fraction and plotted against the NS/M-binding as determined in Fig. 4 (Fig. 5B). The excellent correlation between these results from independent assay procedures unequivocally demonstrates that the relative association rates of topo IIβ target sites with the NS/M varies in a wide range. This is a view considerably different from the one in previous reports that topo II action sites are usually very close to the attachment regions.

Binding of topo IIβ-targeted genomic fragments with hnRNP U/SAF-A/SP120

To explore the expected binding between target clones and the NS/M protein hnRNP U/SAF-A/SP120, we set up two assay systems using magnetic beads conjugated with recombinant SP120. In one system, whole plasmid DNA cut at insertion sites with restriction enzymes was incubated with SP120 immobilized on magnetic beads. The bead-bound DNA and input DNA were separated by agarose gel electrophoresis and quantified (Fig. 6A). It is worth noting that the vector fragment serves as a common competitor against various inserts. The fushitarazu S/MAR, a classical S/MAR isolated from the *Drosophila Ftz* gene upstream [Gasser and Laemmli, 1986; Tsutsui et al., 1993], showed a significant binding with SP120 while non- S/MAR control fragments of various origins did not bind at all. Thus, the reciprocal binding between vector and inserts observed here clearly discriminate S/MAR from non-S/MAR with considerable sensitivity. An extensive analysis with the target plasmids gave basically the same results in that all the insert fragments were favored over vector fragments (Fig. 6B). Interestingly, only the longest fragment was bound when inserts generated multiple fragments, implying that a ‘winner-take-all’ mechanism is involved in the selective binding.

Since the binding of all-or-none fashion prevents further quantitative analysis, we tried another approach in that labeled target fragments were incubated with SP120-beads in the presence of unlabeled competitor DNA (Fig. 6C). This procedure enabled us to evaluate relative affinities of target clones to SP120 (Fig. 6D). In contrast to the binding with NS/M, a large proportion of topo IIβ targets showed significant binding with SP120. Levels of the binding distributed in a narrow range (20-30% of input). Taken together, these results are consistent with the notion that topo IIβ-targeted genomic regions always accompany SP120-binding sites, implying their close relationship. The affinity toward NS/M, however, may be determined by additional factor(s) such as a small difference in the A/T-patch coverage rates (Fig. 4D).

Plausible mechanism for the recognition of S/MAR by topo IIβ/SP120

It has been for some time since both topo II isoforms were demonstrated to be quite mobile in the nucleus of live cells [Christensen et al., 2002]. We reported recently that subnuclear distribution of topo IIβ *in vivo* is determined by its catalytic activity as it shuttles between an active form in the nucleoplasm and a quiescent form in the nucleolus in a dynamic equilibrium [Onoda et al., 2014]. The enzyme is inhibited by RNA that binds to its C-terminal domain and nucleolar RNA appears to tether the enzyme to the nucleolus in an inactive state. It would be reasonable to assume that the nucleoplasmic topo IIβ also stays in a repressed state unless the inhibitory effect of RNA is removed by some factor(s). At present, SP120 is the likeliest candidate for such factors since the protein abolishes the inhibition by RNA by forming an RNA-dependent stoichiometric complex with topo IIβ [Kawano et al., 2010]. Although it remains to be demonstrated, we speculate that topo IIβ/SP120 molecular complex interacts preferentially with AT-rich gene-poor genomic regions, which is consistent with the topo IIβ target clones obtained in the present study and the frequent occurrence of SP120-binding sites in the target clones.

In a recent view, NS/M is also a dynamic entity [Tsutsui et al., 2005; Malyavantham et al., 2010; Razin et al., 2013]. Biochemical composition of NS/M preparations differs depending on both the cellular physiological states and the procedure of isolation. When viewed from the perspective of DNA, S/MAR is not always associated with the isolated NS/M. This is probably because it moves among subnuclear compartments depending

on the transient interaction with proteins, including topo IIβ/SP120. A wide-range distribution of the affinity toward the NS/M observed with topo IIβ target regions may reflect this effect (Fig. 5B). It is worth noting that RNA is the common factor mediating the interaction between topo IIβ/SP120 and also an essential component for the stable isolation of the NS/M [Nickerson et al., 1989].

The binding between SP120 and S/MAR has been shown to involve a great deal of cooperative mechanism [Tsutsui et al., 1993]. The all-or-none binding mode (winner-take-all mechanism) observed in Fig. 6 is most likely to be based on the cooperative interaction facilitated by the immobilization of SP120 on the bead surface. Similar effect of immobilization has been observed in a previous report [Kipp et al., 2000]. This effect may be further amplified by the multiple contacts with the test sequences. The cooperativity might be operating in a larger scale, too. Although it needs to be determined, LAIRs harboring a topo IIβ target could have multiple target sites with cooperative interactions.

We recognized the A/T-patch motif originally in S/MAR sequences and showed that clustering of A/T-patches is an important factor for association with the NS/M [Okada et al., 1996]. We have further demonstrated using artificial DNA oligomers that A/T-patches are also involved in the binding with SP120 and that the affinity is very sensitive to the arrangement of A/T-patches in the oligomers with identical nucleotide composition [Tsutsui, 1998]. Therefore, the frequent occurrence of A/T-patches in topo IIβ targets found in the present study suggests strongly that A/T-patch is a sequence motif mediating the interaction of topo IIβ and SP120 with the NS/M.

ACKNOWLEDGMENT

We thank Kazuko Kiyama for technical assistance. None of the authors have a conflict of interest in regard to this study.

REFERENCES

Chavali PL, Funa K, Chavali S. 2011. Cis-regulation of microRNA expression by scaffold/matrix-attachment regions. Nucleic Acids Res 39:6908-6918.

Christensen MO, Larsen MK, Barthelmes HU, Hock R, Andersen CL, Kjeldsen E, Knudsen BR, Westergaard O, Boege F, Mielke C. 2002. Dynamics of human DNA topoisomerases IIalpha and IIbeta in living cells. J Cell Biol 157:31-44.

Cockerill PN, Garrard WT. 1986. Chromosomal loop anchorage of the kappa immunoglobulin gene occurs next to the enhancer in a region containing topoisomerase II sites. Cell 44:273-282.

Dechering KJ, Cuelenaere K, Konings RN, Leunissen JA. 1998. Distinct frequency-distributions of homopolymeric DNA tracts in different genomes. Nucleic Acids Res 26:4056-4062.

Gasser SM, Laemmli UK. 1986. Cohabitation of scaffold binding regions with upstream/enhancer elements of three developmentally regulated genes of D. melanogaster. Cell 46:521-530.

Iarovaia OV, Akopov SB, Nikolaev LG, Sverdlov ED, Razin SV. 2005. Induction of transcription within chromosomal DNA loops flanked by MAR elements causes an association of loop DNA with the nuclear matrix. Nucleic Acids Res 33:4157-4163.

Ju BG, Lunyak VV, Perissi V, Garcia-Bassets I, Rose DW, Glass CK, Rosenfeld MG. 2006. A topoisomerase IIbeta-mediated dsDNA break required for regulated transcription. Science 312:1798-1802.

Kawano S, Miyaji M, Ichiyasu S, Tsutsui KM, Tsutsui K. 2010. Regulation of DNA Topoisomerase IIbeta through RNA-dependent association with heterogeneous nuclear ribonucleoprotein U (hnRNP U). J Biol Chem 285:26451-26460.

Kipp M, Gohring F, Ostendorp T, van Drunen CM, van Driel R, Przybylski M, Fackelmayer FO. 2000. SAF-Box, a conserved protein domain that specifically recognizes scaffold attachment region DNA. Mol Cell Biol 20:7480-7489.

Lyu YL, Lin CP, Azarova AM, Cai L, Wang JC, Liu LF. 2006. Role of topoisomerase IIbeta in the expression of developmentally regulated genes. Mol Cell Biol 26:7929-7941.

Malyavantham KS, Bhattacharya S, Berezney R. 2010. The architecture of functional neighborhoods within the mammalian cell nucleus. Adv Enzyme Regul 50:126-134.

Mirkovitch J, Mirault ME, Laemmli UK. 1984. Organization of the higher-order chromatin loop: specific DNA attachment sites on nuclear scaffold. Cell 39:223-232.

Nickerson JA, Krochmalnic G, Wan KM, Penman S. 1989. Chromatin architecture and nuclear RNA. Proc Natl Acad Sci U S A 86:177-181.

Okada S, Tsutsui K, Tsutsui K, Seki S, Shohmori T. 1996. Subdomain structure of the matrix attachment region located within the mouse immunoglobulin kappa gene intron. Biochem Biophys Res Commun 222:472-477.

Onoda A, Hosoya O, Sano K, Kiyama K, Kimura H, Kawano S, Furuta R, Miyaji M, Tsutsui K, Tsutsui KM. 2014. Nuclear dynamics of topoisomerase IIbeta reflects its catalytic activity that is regulated by binding of RNA to the C-terminal domain. Nucleic Acids Res 42:9005-9020.

Perillo B, Ombra MN, Bertoni A, Cuozzo C, Sacchetti S, Sasso A, Chiariotti L, Malorni A, Abbondanza C, Avvedimento EV. 2008. DNA oxidation as triggered by H3K9me2 demethylation drives estrogen-induced gene expression. Science 319:202-206.

Razin SV, Gavrilov AA, Ioudinkova ES, Iarovaia OV. 2013. Communication of genome regulatory elements in a folded chromosome. FEBS Lett 587:1840-1847.

Romig H, Fackelmayer FO, Renz A, Ramsperger U, Richter A. 1992. Characterization of SAF-A, a novel nuclear DNA binding protein from HeLa cells with high affinity for nuclear matrix/scaffold attachment DNA elements. EMBO J 11:3431-3440.

Sano K, Miyaji-Yamaguchi M, Tsutsui KM, Tsutsui K. 2008. Topoisomerase IIbeta activates a subset of neuronal genes that are repressed in AT-rich genomic environment. PLoS One 3:e4103.

Sato A, Sekine Y, Saruta C, Nishibe H, Morita N, Sato Y, Sadakata T, Shinoda Y, Kojima T, Furuichi T. 2008. Cerebellar development transcriptome database (CDT-DB): profiling of spatio-temporal gene expression during the postnatal

development of mouse cerebellum. Neural Netw 21:1056-1069.

Tsutsui K. 1998. Synthetic concatemers as artificial MAR: importance of a particular configuration of short AT-tracts for protein recognition. Gene Therapy and Molecular Biology 1:581-590.

Tsutsui K, Tsutsui K, Hosoya O, Sano K, Tokunaga A. 2001a. Immunohistochemical analyses of DNA topoisomerase II isoforms in developing rat cerebellum. J Comp Neurol 431:228-239.

Tsutsui K, Tsutsui K, Muller MT. 1988. The nuclear scaffold exhibits DNA-binding sites selective for supercoiled DNA. J Biol Chem 263:7235-7241.

Tsutsui K, Tsutsui K, Okada S, Watarai S, Seki S, Yasuda T, Shohmori T. 1993. Identification and characterization of a nuclear scaffold protein that binds the matrix attachment region DNA. J Biol Chem 268:12886-12894.

Tsutsui K, Tsutsui K, Sano K, Kikuchi A, Tokunaga A. 2001b. Involvement of DNA topoisomerase IIbeta in neuronal differentiation. J Biol Chem 276:5769-5778.

Tsutsui KM, Sano K, Tsutsui K. 2005. Dynamic view of the nuclear matrix. Acta Med Okayama 59:113-120.

FIGURE LEGENDS

Fig. 1. Expression of topo IIβ in the rat cerebellar cortex at 10 days after birth (P10). Cryosections (10 μm) were immunostained with anti-topo IIβ monoclonal antibody, followed by Texas Red-X-conjugated secondary antibody (shown in the middle panel). DNA was stained simultaneously with 4',6-diamidino-2-phenylindole (DAPI) and observed on a fluorescence microscope. Identity of cortical layers is designated on the right. EGL, external germinal layer; ML, molecular layer; PL, Purkinje cell layer; GL, granular layer. Scale bar=20 μm. Arrowheads indicate Purkinje cell nuclei.

Fig. 2. Topo IIβ targets reside in genomic regions of extremely low GC content. (A) Histogram of GC content distribution. For the genome, GC content was calculated for non-overlapping 3 kb-segments originated from the whole genome. Mean GC contents were 0.35 for the 279 targets and 0.42 for whole genome. (B) Patch size dependency of A/T-patch coverage rates (%). A/T-patch coverage is defined as 100 $(n[A]_n + n[T]_n)/([A]+[T]+[G]+[C])$, where $[A]_n$ is the number of A-tract with length 'n', $[T]_n$ is the number of T-tract with length 'n', and $[A]$, $[T]$, $[G]$, $[C]$ are base counts in the sequence. The genome control was composed of 300 samples of randomly selected 3 kb-fragments. A/T-patch coverage (%) at patch size 'n' was box-plotted using the program 'R' with default settings. (C) Determination of the optimal A/T-patch size that can discriminate target clones from the genome. A/T-patches of length 'n' (n, varied from 1 to 8) were identified in target sequences and in genome samples to calculate their coverage rates in the sequence. The difference between the two groups was verified statistically by Mann-Whitney test. The reciprocal of log (*P*-value) was plotted against 'n'. (D) Comparison of A/T-patch coverage rates between target clones and genome samples. A/T patches are combined and defined as below.

$$\text{A/T-patch coverage } (\%) = 100 \sum_{n=2}^{5} \left(n[A]_n + n[T]_n\right) / \left([A]+[T]+[G]+[C]\right)$$

A/T-patch coverage of each group was box-plotted as in Fig. 2B. $P<3\text{x}10^{-52}$ (Mann-Whitney).

Fig. 3. Topo IIβ targets occupy a unique position in the genome. (A) The target clones are frequently located in intergenic regions. Genomic positions of 279 target clones were determined by Blat search and assigned to genic/intergenic regions of modified RefSeq database (exRefSeq). Partition rates of target clones (closed bars) and genomic coverage rates (open bars) are plotted simultaneously as relative values. GR, genic region; IR, intergenic region. (B) Preferred location of target clones in classified intergenic regions. Average values were used for class limits: GC content (0.42), length (110 kb). Relative values are plotted. L and S stand for long and short with respect to the average, respectively. *P*-value, from chi-square test. (C) The long and AT-rich intergenic region (LAIR) targeted by topo IIβ is frequently juxtaposed to long and AT-rich genes. Genomic positions for LAIRs containing mapped target clones (N=195) and LAIRs in the whole genome (N=1189) were first identified. Percentages of LAIRs with juxtaposed long and AT-rich genes were then compared between the two groups. *P*-value, from chi-square test.

Fig. 4. Specific interaction of the target fragments with the NS/M. (A) Assessment of conditions for the binding. Representative plasmids selected from the target library were used (clone numbers at the top). Concentrations of the competitor *E. coli* DNA added to the reaction were 0, 0.2, 0.4, and 0.8 mg/ml (from the left). pAR1 was digested with *Bam*HI and *Hin*dIII to liberate the insert (mouse Igκ MAR). NS/M-bound DNA fragments were separated by polyacrylamide gel electrophoresis and visualized by autoradiography. Arrowheads indicate vector fragments. (B) Analysis of 37 target clones. Clones with short inserts (< 300 bp) were omitted. The competitor concentration was fixed at 0.4 mg/ml of *E. coli* DNA. Numbers stand for the clone number. For each clone, the binding reaction was performed in the absence (left lanes) or presence (right lanes) of the competitor DNA. Arrowheads indicate vector fragments. (C) A histogram of relative affinities of target clones. Autoradiograms shown in B were scanned and the % NS/M-binding was calculated for each as described in Methods (tabulated in Table S1). When multiple fragments were generated from the insert, the fragment with the highest binding was used for assignment. (D) Correlation between the NS/M-binding and the A/T-patch coverage rates. The correlation coefficient (R=0.472) was statistically significant by Student t-test (P<0.01).

Fig. 5. PCR-based matrix/loop partition assay. (A) Relative band intensity of PCR products plotted against the cycle number. The ratio of copy numbers in matrix versus loop fractions (M/L) is presented for only representative clones but the complete M/L data are given in Table S1. (B) Correlation plot for the two methods used in the matrix-association studies. Abscissa, %NS/M-binding from the assay shown in Fig. 4; ordinate, %matrix-association from the matrix/loop partition assay. Representative target clones shown in A are indicated in the figure. R, correlation coefficient**.**

Fig. 6. Selective binding of target clones to SP120 immobilized on magnetic beads. (A) A pilot experiment to test the selectivity of the binding. The control non-S/MAR DNAs used are cDNA clones of rat GABA-A receptor α1/ α6, engrailed gene (EN2), and random clones of *E. coli* DNA. The extra band in GABAAα6 is generated by a cleavage in the insert. I, input; B, bound. Arrowheads indicate vector fragments. (B) Binding of the target clones. Plasmids were cut with *Eco*RI/*Xho*I and analyzed as in A. Arrowheads indicate vector fragments. (C) Schematic representation of the binding assay with fluorescence-labeled DNA fragments. (D) Frequency distribution of the affinity between SP120 and target clones (analyzed as in C).

Fig.1

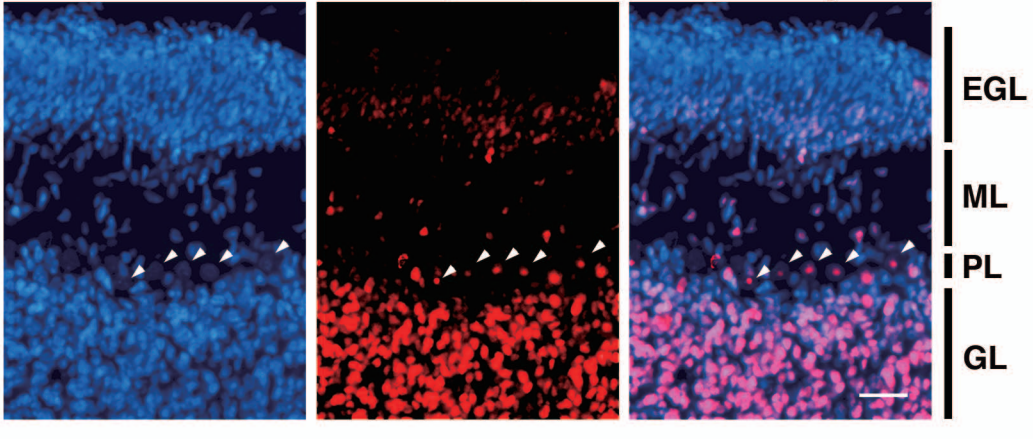

Fig.2

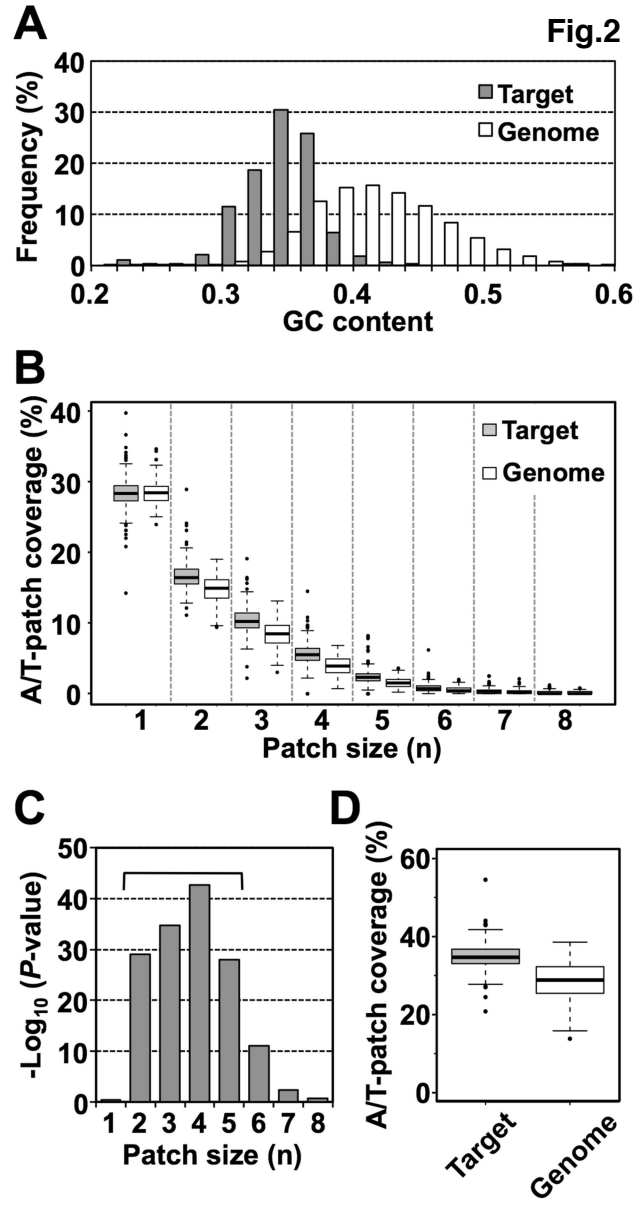
A
Frequency (%)
40
30
20
10
0
Target
Genome
0.2
0.3
0.4
0.5
0.6
GC content
B
A/T-patch coverage (%)
40
30
20
10
0
Target
Genome
1
2
3
4
5
6
7
8
Patch size (n)
C
-Log10 (P-value)
50
40
30
20
10
0
1
2
3
4
5
6
7
8
Patch size (n)
D
A/T-patch coverage (%)
60
40
20
0
Target
Genome

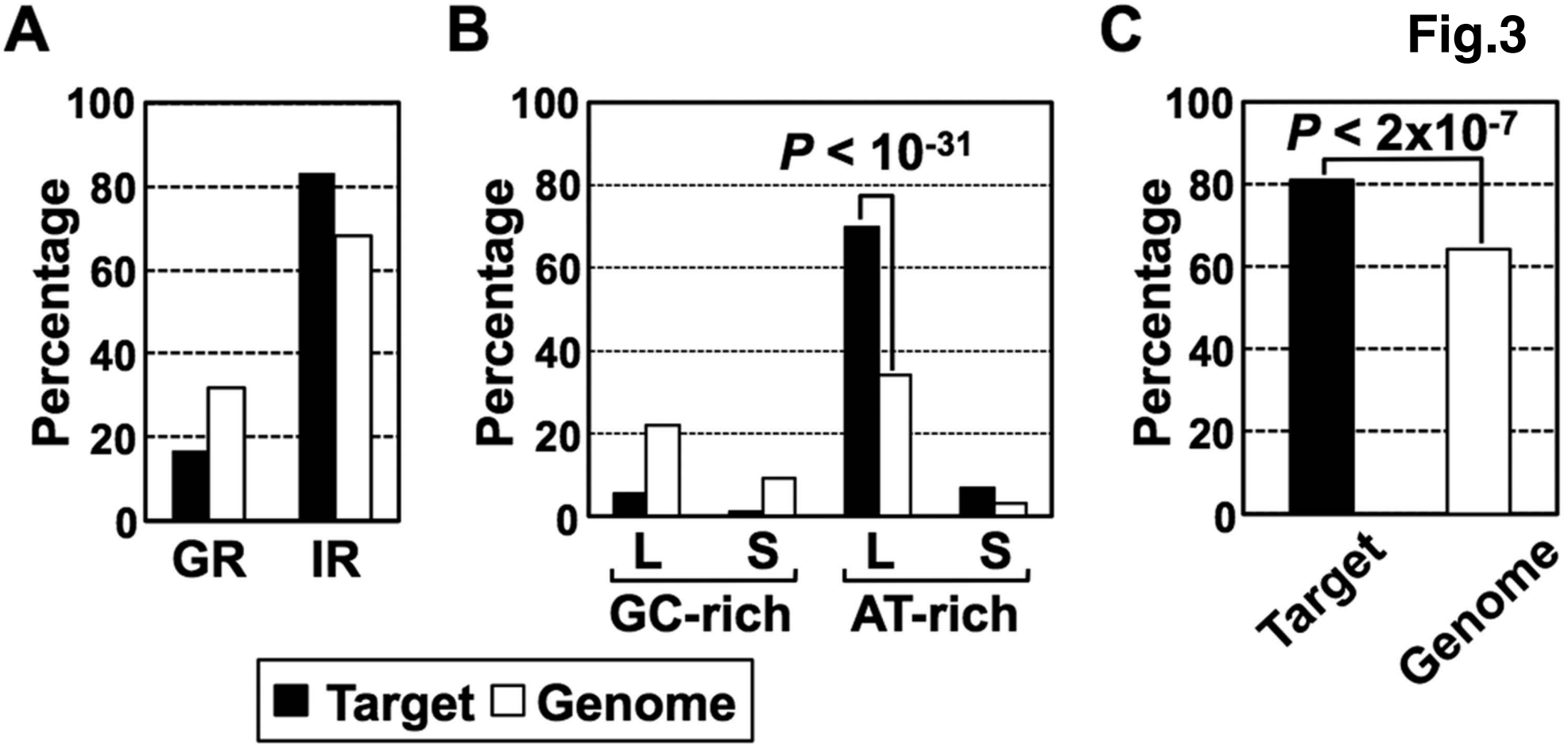
A
B
C
Fig.3
Percentage
100
80
60
40
20
0
GR
IR
P < 10-31
L
S
GC-rich
AT-rich
P < 2x10-7
Target
Genome
Target
Genome

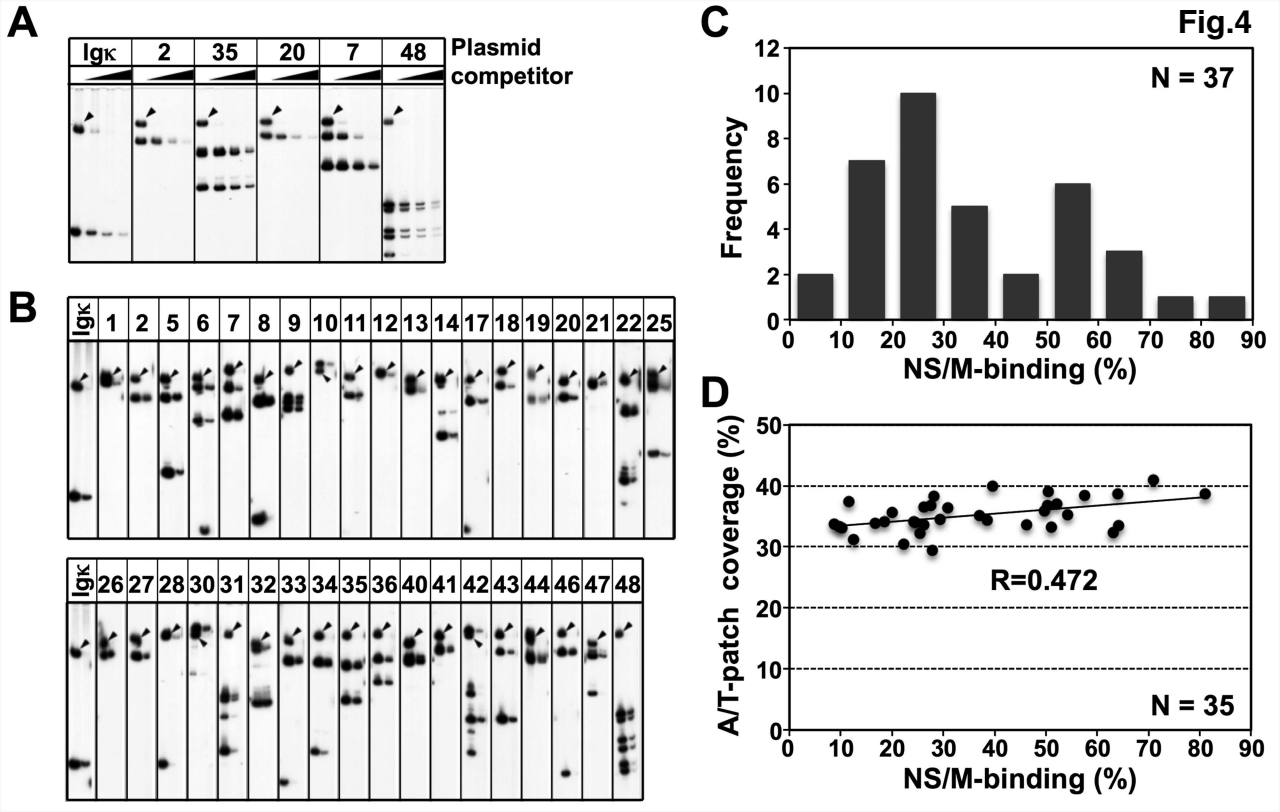
A
Igκ
2
35
20
7
48
Plasmid competitor
B
Igκ
1
2
5
6
7
8
9
10
11
12
13
14
17
18
19
20
21
22
25
Igκ
26
27
28
30
31
32
33
34
35
36
40
41
42
43
44
46
47
48
C
Fig.4
N = 37
Frequency
NS/M-binding (%)
D
A/T-patch coverage (%)
R=0.472
N = 35
NS/M-binding (%)

Fig.5

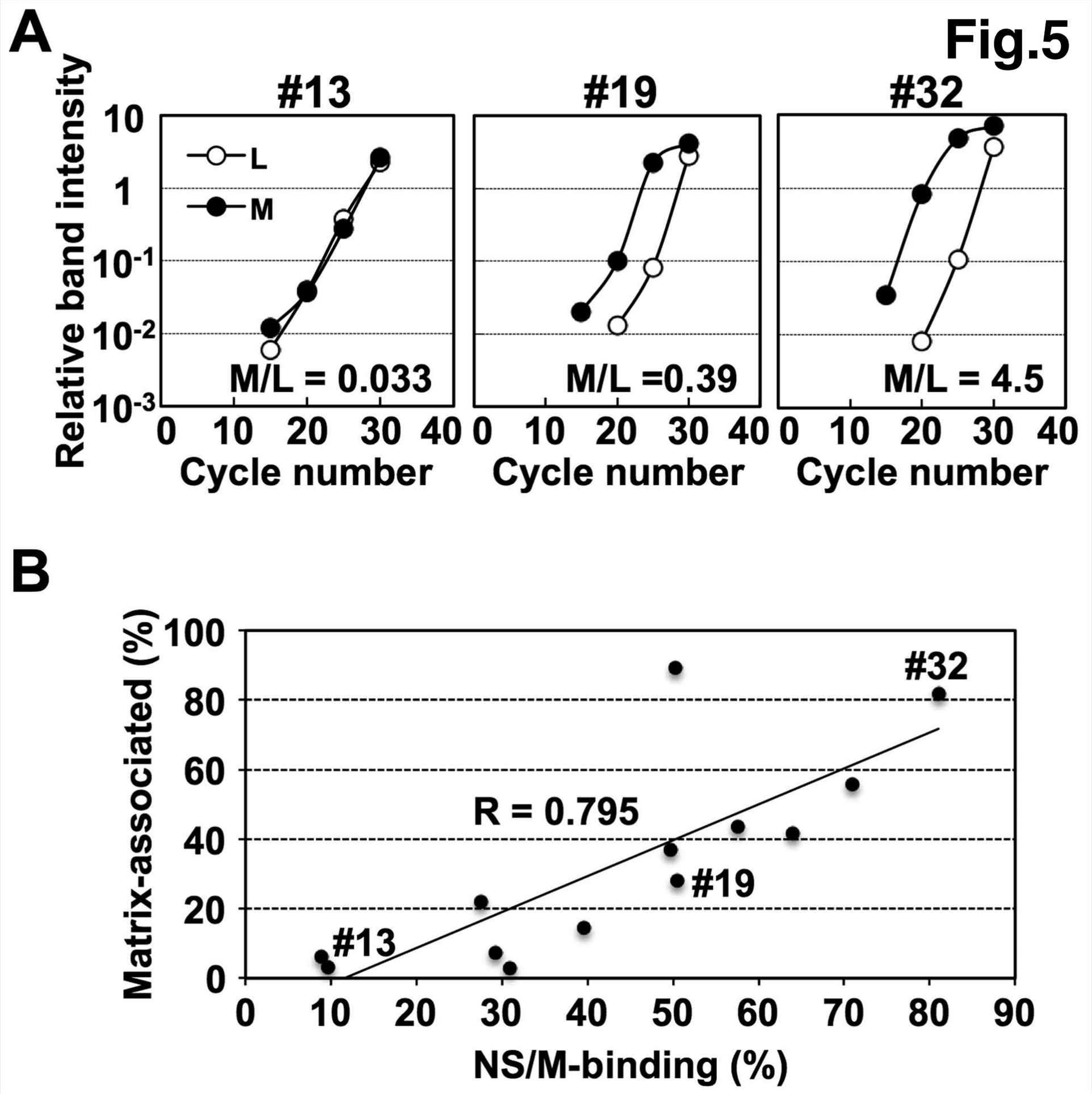
A
#13
#19
#32
L
M
Relative band intensity
10
1
10-1
10-2
10-3
M/L = 0.033
M/L =0.39
M/L = 4.5
0 10 20 30 40
Cycle number
B
Matrix-associated (%)
100
80
60
40
20
0
R = 0.795
#13
#19
#32
0 10 20 30 40 50 60 70 80 90
NS/M-binding (%)

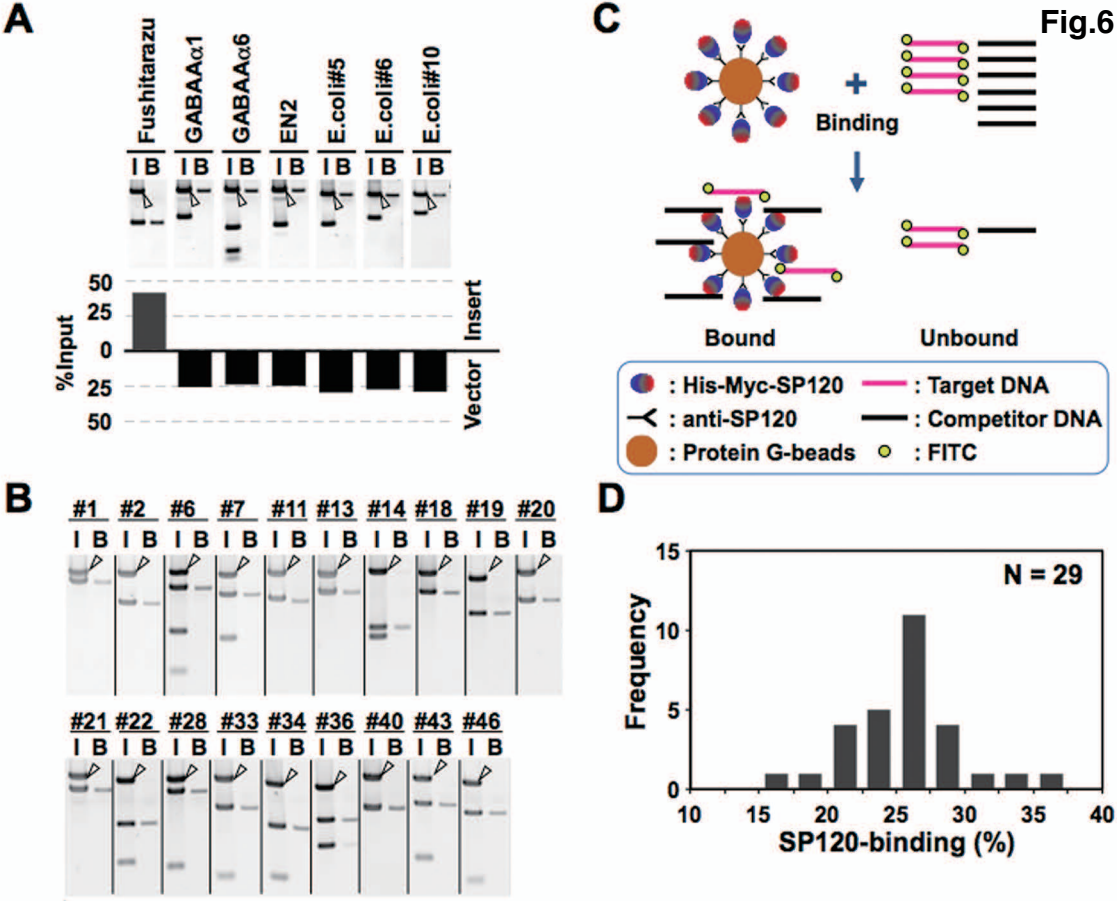
A
Fushitarazu
GABAAα1
GABAAα6
EN2
E.coli#5
E.coli#6
E.coli#10
I B
50
25
0
25
50
%Input
Insert
Vector
B
#1 #2 #6 #7 #11 #13 #14 #18 #19 #20
#21 #22 #28 #33 #34 #36 #40 #43 #46
C
Binding
Bound
Unbound
: His-Myc-SP120
: anti-SP120
: Protein G-beads
: Target DNA
: Competitor DNA
: FITC
D
N = 29
Frequency
SP120-binding (%)
0
5
10
15
10
15
20
25
30
35
40

Supporting Data

Genomic regions targeted by DNA topoisomerase IIβ frequently interact with a nuclear scaffold/matrix protein hnRNP U/SAF-A/SP120

Mary Miyaji*[,1], Ryohei Furuta[1], Kuniaki Sano, Kimiko M. Tsutsui, and Ken Tsutsui*
Department of Neurogenomics, Graduate School of Medicine, Dentistry and Pharmaceutical Sciences, Okayama University, 2-5-1 Shikata-cho, Kita-ku, Okayama 700-8558, Japan

[1]These authors equally contributed to this work.

*Corresponding authors:
Department of Neurogenomics, Graduate School of Medicine, Dentistry and Pharmaceutical Sciences, Okayama University, 2-5-1 Shikata-cho, Kita-ku, Okayama 700-8558, Japan. Phone: +81-86-235-7097, Fax: +81-86-235-7103.
E-mail: tsukken@cc.okayama-u.ac.jp (K.T.), mmiyaji@md.okayama-u.ac.jp (M.M.)

Table S1

Clone ID	Mapping	Chr	Start	End	Length (bp)	GC (%)	SP120-binding (%Input)	NS/M-binding (%Input)	M/L ratio	Foward primer sequence (5'-3')	Reverse primer sequence (5'-3')
#01	U	14	102,852,710	102,855,514	2,805	41.9	21.6	12.5			
#02	U	3	26,730,820	26,733,974	3,155	38.2	16.7	49.7	0.59	TCAGCCAGATTTGGGGTCTT	GCATTTTAATAGAAGCTGTGAGG
#03	M	-	-	-	-	-					
#04	U	X	130,559,431	130,559,479	49	37.3					
#05	U	16	68,365,930	68,368,193	2,264	39.7					
#06	N	-	-	-	3,734	33.1		37.1			
#07	U	8	90,204,905	90,208,032	3,128	38.1		63.1			
#08	U	5	113,004,249	113,008,038	3,790	36.5	23.2	64.2			
#09	U	1	57,236,745	57,240,454	3,710	37.2	26.5	46.3			
#10	U	1	92,197,167	92,200,648	3,482	42.5	22.1	11.6			
#11	U	4	24,480,174	24,482,833	2,660	39.5	27.8	38.5			
#12	U	20	34,599,488	34,602,775	3,288	38.2	23.1	20.0			
#13	U	2	81,782,381	81,784,735	2,355	38.2	20.7	9.7	0.033	GGCATGGAGGAGAAAAAACT	GAAGGCAGCAAATACTTTCC
#14	U	14	60,906,413	60,908,241	1,829	37.5	26.1	27.6	0.28	GATTGTCTATAAGCAAGTCTG	AAAATAGTATACTGAGTATCTTGG
#15	O										
#16	U	3	97,318,754	97,318,944	191	38.0					
#17	U	X	15,130,388	15,132,447	2,060	39.5	29.4	22.3			
#18	U	13	9,336,314	9,338,551	2,238	38.0	19.3	8.8	0.067	GGCCTGAAAACTTTACTCAG	CCTGTGCTCAGGTTTGTAAA
#19	U	11	19,999,742	20,001,361	1,620	36.9	30.5	50.5	0.39	AGTCAAGTACCCATCCCTA	GAAAACTTCCTAATCTGGCAC
#20	U	8	42,970,787	42,973,183	2,397	38.7	27.0	24.5			
#21	U	4	89,035,578	89,038,137	2,560	37.2	28.4	28.1			
#22	U	10	23,508,185	23,509,955	1,771	38.9		50.3	8.3	CGATATTGCTTCCAGAAAAAG	AAACTTTGATATGGAATGAATTCC
#23	U	15	29,883,825	29,883,962	138	41.6					
#24	O										
#25	U	3	82,973,677	82,976,764	3,088	37.6	26.3	18.6			
#26	U	15	64,361,641	64,363,280	1,640	36.1	24.6	71.0	1.3	GATCTGCTCATTTCTTTGAG	GATTAATATGGGCAGCCTTT
#27	U	2	132,599,783	132,601,663	1,881	36.8	24.1	26.2			
#28	U	1	63,278,551	63,281,454	2,904	38.9	25.2	10.2			
#29	O										
#30	U	15	49,201,489	49,204,655	3,167	39.8					
#31	M	-	-	-	-	-					
#32	U	16	34,538,218	34,541,579	3,362	37.6	25.3	81.0	4.5	GATCACTGCTCACTTTAATG	ATTTTCGATCTAGCAAGTGG
#33	N	-	-	-	2,208	35.5	26.3	29.3	0.079	GCATGCTGTCAAAAGTTAAAAATAC	TGAAAGTGCATCCCGATCTT
#34	U	6	56,906,209	56,908,024	1,816	37.5	25.1	64.0	0.71	GTGCTCACAATTGCTGTTAG	TAGCCTGAGTGACAAAGTGA
#35	N	-	-	-	1,926	32.8	22.8	57.5	0.77	CTAGAGAATTCACAATATAAAGG	TAAAGTTATAGCTCATCATGAC
#36	U	4	143,247,525	143,250,285	2,761	39.4	21.8	51.1			
#37	O										
#38	O										
#39	O										
#40	U	6	21,155,160	21,157,009	1,850	36.4	33.7	39.6	0.17	ACAAAAAGAAGGAGCTTGGC	GCAAGAGCTACATTGTAAGG
#41	U	18	21,070,180	21,072,495	2,316	38.4	25.2	24.2			
#42	U	2	221,406,559	221,412,324	5,766	38.6					
#43	N	-	-	-	2,562	34.2	27.4	26.2			
#44	U	9	95,063,599	95,065,531	1,933	38.5	27.9	30.9	0.029	GTGATCAACTTGTGCATGAG	TTGACCTGTTAAGGTCTAGG
#45	O										
#46	U	13	27,330,915	27,333,480	2,566	37.8	36.3	52.2			
#47	U	4	20,608,279	20,609,861	1,583	37.6	26.3	16.7			
#48	M	-	-	-	-	-		30.1			

Table S1. Summary of topo IIβ target clones used for analyses. Mapping: U, uniquely mapped; M, multiply mapped; N, not mapped (position unknown); O, omitted from the analysis (no insert, duplicated clones, etc.). Chr, chromosome number; Start/End, nucleotide positions of cloned fragments on rat genome (rn3); Length (bp), fragment length of insert; GC (%), GC content. SP120-binding, fluorescent probe bound to immobilized SP120 (% of input); NS/M-binding, labeled fragment bound to the NS/M (% of input); M/L ratio, ratio of copy numbers found in matrix versus loop fractions. Shown in the last 2 columns are sequences for the clone-specific primer pairs used for the matrix-loop partitioning assay.

Figure S1

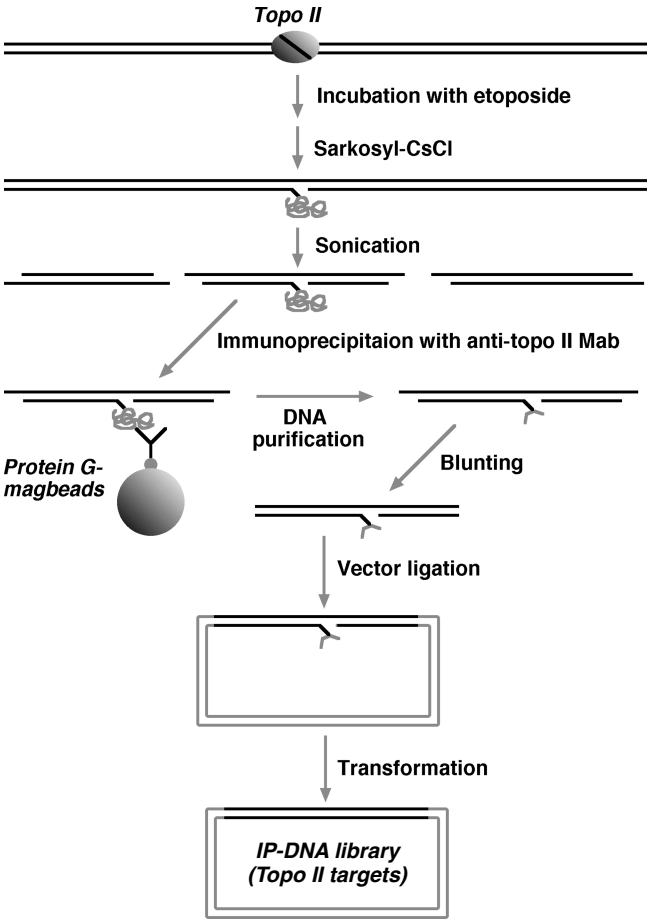

Figure S1. Outline for the construction strategy of a library of genomic DNA fragments targeted by topo IIβ *in vivo*.

Figure S2

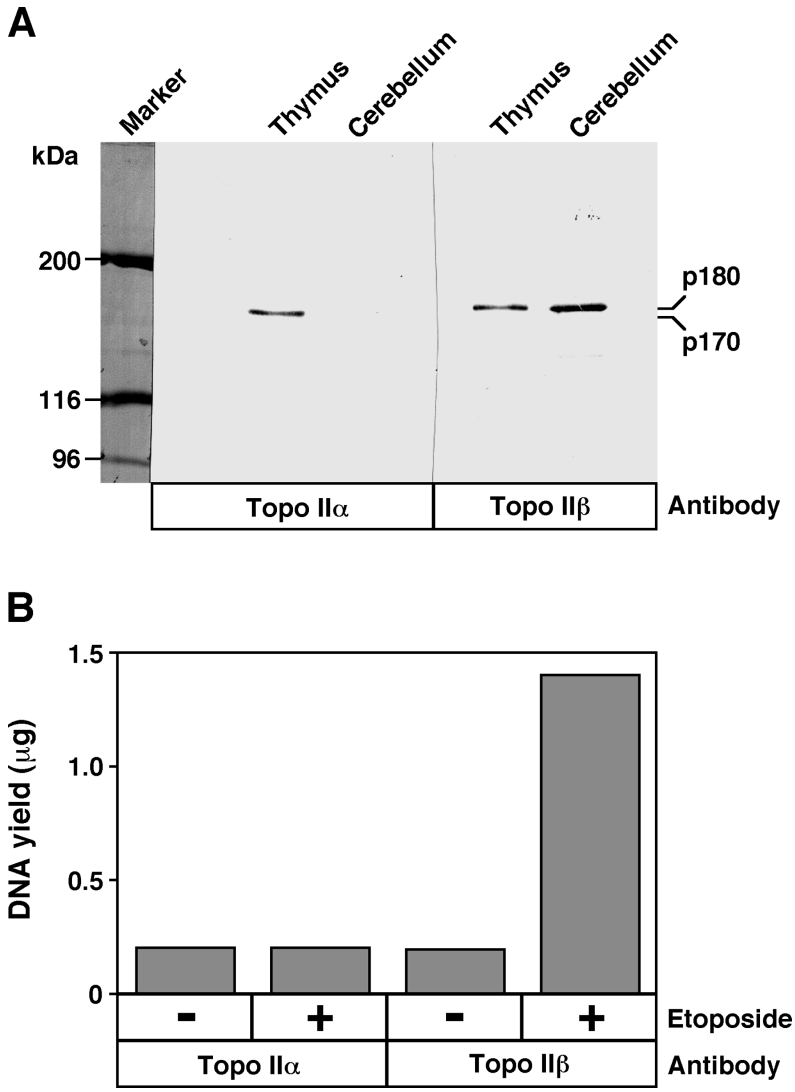

Figure S2. Evidence for successful isolation of genomic fragments targeted by topo IIβ. (A) Immunoblotting of tissue extracts with isoform-specific monoclonal antibodies. Thymus tissue was used as a control in which both topo II isoforms are expressed. p170, topo IIα; p180, topo IIβ. (B) Amounts of DNA recovered from cerebellar tissue lysates after the immunoselection procedure with isoform-specific antibodies. The DNA yield shown here is obtained from materials equivalent to a half cerebellum (~35 mg wet weight). Before lysis, tissue slices were preincubated in a medium with (+) or without (-) 100 μM etoposide.

Figure S3

Fig. S3. Highlighting the A/T-patches in a topo IIβ target clone sequence (#26, 1,640 bp). Short A/T tracts were identified and highlighted in magenta (A-patch) or in green (T-patch). For the calculation of patch coverage rates according to the formula shown on the bottom, only patch sizes n=2,3,4,5 were taken into account (underlined). For reference, the A/T-patch coverage rate of this sequence is 41%.

$$\text{A/T-patch coverage } (\%) = 100 \sum_{n=2}^{5} \left(n[A]_n + n[T]_n \right) / \left([A]+[T]+[G]+[C] \right)$$